

# Analysis of the MFRSR Data from SGP and NYC Sites

*M. D. Alexandrov, A. A. Lacis, B. E. Carlson, and B. Cairns*  
*NASA-Goddard Institute for Space Studies*  
*New York, New York*

## Introduction

Aerosols can affect the climate both directly and indirectly and are considered to be the largest source of uncertainty in defining the anthropogenic contribution to global radiative forcing of climate during the past century, and of the projected forcing of climate change in the future. Satellite measurements with sufficient accuracy to monitor the climatic forcing by aerosols [except for the Stratospheric Aerosol and Gas Experiment (SAGE II) measurements of volcanic aerosols] will not be available for years to come; thus, it is important to make better use of those measurements that are currently available. Multi-filter rotating shadowband radiometer (MFRSR) measurements, which have been available since the beginning of operations, are one such example of a potentially very important but underutilized data set.

## Analysis

The MFRSR makes precise simultaneous measurements of the direct solar beam extinction, and horizontal diffuse flux, at six wavelengths (nominally 415 nm, 500 nm, 615 nm, 670 nm, 870 nm, and 940 nm) at 1-minute intervals throughout the day (Harrison et al. 1994).

The atmospheric column extinction optical depth corresponding to the  $i^{\text{th}}$  channel can be expressed in terms of the parameters measured by MFRSR as  $\tau_i = -\ln(I_i/I_i^0) \cdot c_i \mu$ , where  $\mu$  is the cosine of the solar zenith angle,  $I_i^0$  are the top of the atmosphere solar radiation intensities, and  $c_i$  are the natural logarithms of the respective calibration coefficients that convert measured detector voltages to intensities in  $\text{Wm}^{-2}$ . In this paper, we use the name “calibration coefficients” for the coefficients  $c_i$ .

Besides water vapor at 940 nm (which is not a subject of this study), the other gaseous absorbers within the MFRSR channels are  $\text{NO}_2$  (at 415 nm, 500 nm, and 615 nm) and  $\text{O}_3$  (at 500 nm, 615 nm, and 670 nm). Aerosols and Rayleigh scattering contribute atmospheric extinction in all MFRSR channels. The absorption coefficients for  $\text{NO}_2$  and  $\text{O}_3$  are

accurately known, and the aerosol spectral extinction is strongly constrained (for given refractive index and particle size) by Mie scattering.

Given the unique spectral signature of each atmospheric constituent, retrievals can be obtained simultaneously point-by-point to provide the daily time series of aerosol,  $\text{NO}_2$ , and  $\text{O}_3$  variability. However, there is a persistent problem with MFRSR calibration stability that can seriously impact retrieval credibility, in addition to the fact that the commonly used Langley calibration method is reliable only for the days when the optical depth does not change; often that is not the case.

We proposed an algorithm (Alexandrov et al. 1997) that allows us to overcome the calibration problems and accurately retrieve column  $\text{NO}_2$ , ozone, the aerosol optical depth (AOD), and column mean particle size. This retrieval algorithm consists of the following steps:

1. determination of the calibration coefficient together with the AOD and the single scattering albedo in the fifth channel (870 nm) by comparison of the optical depth obtained from the direct beam intensity with the one retrieved from the direct to diffuse ratios
2. separation of the aerosol extinction from other factors by analytical solution of the system of linear (in AOD and gases column amounts) equations, determination of the aerosol size distribution parameters, calculations of the AODs in all channels using the results of Mie theory
3. retrieval of  $\text{NO}_2$  and ozone column amounts (together with the calibration coefficients in the first two channels)
4. determination of the remaining calibration coefficients.

To model the diffuse flux in the first step, multiple scattering calculations were performed using the doubling and adding method. We restrict our consideration to the fifth (870 nm) channel, only because this channel is not

affected by  $\text{NO}_2$  and ozone absorption; hence, the computational results do not depend on the unknown vertical distribution of these gases.

Comparison of the AOD  $\tau_5$  obtained from the direct beam intensity only with the one calculated by inversion of the formula (King and Herman 1979) relating the surface albedo, the direct-to-diffuse ratio corresponding to this albedo and the one corresponding to zero surface reflectivity, shows that the difference between them is linear with respect to  $\mu$ . The constant term in this dependence can be explained by aerosol absorption properties. This offset can be reduced to zero by changing the aerosol single scattering albedo (that itself can be determined by this procedure).

This analysis of the data from the NYC site shows that the assumption of non-absorbing aerosol works very well, while for the Southern Great Plains (SGP) site some handling of the aerosol absorption seems to be necessary. (However, the values of the single scattering albedo required to explain the data appeared to be too low, which may indicate some technical problems with the instrument.)

Underestimation of the aerosol absorption in the retrieval algorithm at hand may lead to overestimation of the  $\text{NO}_2$  column amount (since the difference in extinction between absorbing and non-absorbing aerosols is mostly pronounced in the wavelengths region containing the first channel). Other retrieved physical quantities are not significantly affected by neglecting the absorption. The data presented in this paper was obtained under the assumption of sulfate aerosol ( $n_r = 1.4$ ,  $n_i = 0$ ).

The measured quantities and the quantities to be determined satisfy a system of five equations of the form:

$$\tau_i = q_i \tau_a + \beta_i x_{\text{NO}_2} + \gamma_i x_{\text{O}_3} + c_i \mu, \quad (1)$$

where  $\tau_i$  are the measured optical depths in the  $i^{\text{th}}$  channel;  $q_i = Q_{\text{ext}}^i / Q_{\text{ext}}^5$  are the Mie scattering extinction ratios normalized to the fifth (870 nm) channel (by definition  $q_5 = 1$ );  $\beta_i$  and  $\gamma_i$  are the effective spectral absorption coefficients of  $\text{NO}_2$  and  $\text{O}_3$ , respectively, weighted by the solar flux and filter response function of each respective MFRSR channel (the coefficients  $\beta_5 = 0$ ,  $\gamma_1$  and  $\gamma_5$  are effectively equal to zero);  $x_{\text{NO}_2}$  and  $x_{\text{NO}_3}$  are respective column amounts of  $\text{NO}_2$  and ozone;  $\tau_a$  is the AOD (at 870 nm) in MFRSR channel 5, and  $c_i$  are the calibration coefficients.

By means of a simple algebraic transformation, one can exclude  $x_{\text{NO}_2}$ ,  $x_{\text{NO}_3}$ , and  $\tau_a$  from the system, which then (after division by  $\mu$ ) takes the form:

$$F_3 - B_3(x - c_5) + A_3, \quad F_4 = B_4(x - c_5) + A_4, \quad (2)$$

where  $x = \tau_5 / \mu$ .

$$\begin{aligned} F_i &= \mu^{-1}(\tau_i - b_{i1}\tau_1 - g_{i2}(\tau_2 - b_{21}\tau_1)), \\ A_i &= c_i - b_{i1}c_1 - g_{i2}(c_2 - b_{21}c_1), \\ B_i &= q_i - b_{i1}q_1 - g_{i2}(q_2 - b_{21}q_1). \end{aligned} \quad (3)$$

Here,  $i = 3, 4$ ,  $b_{ij} = \beta_i / \beta_j$ ,  $g_{ij} = \gamma_i / \gamma_j$ . We see that the left-hand sides  $F_i$  of the equations (2) and (3) contain only measured parameters and can thus be calculated directly from the observed data (without modeling assumptions). Meanwhile, the right-hand sides are linear functions of the argument  $x = \tau_5 / \mu$  over any time interval where the aerosol size distribution parameters (and therefore,  $q_i$ ) do not change, and  $F_i = A_i$  when  $x = c_5$  for any value of  $B_i$ . Accordingly, the  $A_i$  represent combinations of calibration coefficients, and are supposed to remain constant during the day. It follows from the above that all points on the plot  $F_i(x)$ , corresponding to the same aerosol size distribution, belong to a straight line with the slope  $B_i$ , passing through the ‘‘calibration point’’ with the coordinates  $(c_5, A_i)$ . Thus, knowing  $c_5$  from the previous step, one can use the Langley-like regressions with the only difference being that we now are dealing with the variability of the aerosol size distribution, which appears to be much more stable than the AOD.

The coefficients  $B_3$  and  $B_4$  obtained in this way, formally depend only on the (unknown) aerosol extinction ratios  $q_i$ . Therefore, formally, they can be used to determine the parameters  $r_{\text{eff}}$  and  $v_{\text{eff}}$  of a pre-assumed aerosol size distribution by using Mie theory (specified refractive index) to calculate the extinction ratios  $q_i$  and then create look-up tables for  $B_3$  and  $B_4$  as functions of  $r_{\text{eff}}$  and  $v_{\text{eff}}$  using Eq. (3). Then, the retrieved  $r_{\text{eff}}$  and  $v_{\text{eff}}$  will be the coordinates of the intersection point of the level curves in  $(r_{\text{eff}}, v_{\text{eff}})$ -plane corresponded to the measured values of  $B_3$  and  $B_4$ . However, in practice, these curves either don’t intersect or the point of their intersection is unreliable (if it is sensitive to the shape of the pre-assumed aerosol size distribution). This means, in general, that as far as the extinction ratios are concerned, the parameters  $r_{\text{eff}}$  and  $v_{\text{eff}}$  are not universal and their numerical values make sense only if the shape of the distribution is accurately known.

However, we find that in the case of relatively small particles with  $r_{\text{eff}} \leq 0.5 \mu\text{m}$ , that frequently occur in observed aerosol size distributions, the curves nearly coincide and can be treated as one curve. In this case, the point of intersection is certainly unreliable, but the position of the curve itself is well-determined and does not significantly depend on the pre-assumed form of the aerosol size distribution shape. We will characterize this curve by the  $r_{\text{eff}}$  corresponding to the reference  $v_{\text{eff}} = 0$ . This, we refer to as “mono-distribution radius” (since it is calculated under the assumption that all aerosol particles have the same size). The mono-distribution radius appears to give accurate information with respect to aerosol extinction properties and its asymmetry parameter.

Once the mono-distribution radius is determined, the AODs in all other channels can then be calculated based on the Mie scattering relationships and then subtracted from the observed extinction data. The remaining optical depth in the first channel is caused by  $\text{NO}_2$  absorption, in the second channel by both  $\text{NO}_2$  and ozone absorption. To separate  $\text{NO}_2$  and ozone absorption from calibration, we use a simple least-squares fit in the first channel, similar to the procedure in the Langley analysis. In the case of ozone, we first analytically exclude  $\text{NO}_2$  contributions from the second channel extinction. The calibration coefficients  $c_1$  and  $c_2$  are determined on this step together with the gases column amounts. Retrieval accuracy for column ozone appears to be much better than for  $\text{NO}_2$ , shows relatively little dependence on the value of  $v_{\text{eff}}$ , and is in good agreement with the Earth Probe total ozone mapping experiment spectrometer (TOMS) measurements.

The remaining calibration coefficients  $c_3$  and  $c_4$  can be obtained (e.g., by direct subtracting of the determined optical depths from the measured ones).

The calibration history of the instrument located at the SGP site in the first year of the MFRSR operation shows that the calibration coefficients are, on average, stable with a small trend from 0.2 to 0.1 during the year. This behavior is quite a contrast to the fast degradation of the Goddard Institute for Space Studies (GISS) MFRSR filters in 1995, and again in 1997 after the re-calibration of the instrument.

Figure 1 summarizes the results obtained with our retrieval analysis for clear and partially clear days from MFRSR measurements taken at the SGP site during 1993. The first two plots show the daily mean AOD (at 550 nm) and the

daily mean aerosol mono-distribution radius for the whole observation period. Polynomial fits to the data show more clearly the seasonal variations of these parameters. We see that the mean AOD in winter is smaller than in summer, while the aerosol particles are bigger. This may be related to changes in condensation and/or evaporation conditions, and is quite understandable: the same mass of a scattering material decomposed into a larger number of smaller particles produces larger optical depth (actually, it is true only for particles with radius greater than  $0.3 \mu\text{m}$ ).

The next two plots on Figure 1 show changes in  $\text{NO}_2$  and ozone column amounts. Ozone amounts are expressed in Dobson units, and column  $\text{NO}_2$  is given in parts per billion relative to the entire air column of  $2.15 \times 10^{25} \text{ mol/cm}^2$ . It is shown here how the accuracy of retrieval is limited by the dependence of the retrieved values on the unknown value of the aerosol size distribution variance  $v_{\text{eff}}$ . Despite the low accuracy of the  $\text{NO}_2$  retrieval, and its high variability, the average values of column  $\text{NO}_2$  given by the polynomial fit, appear to show reasonable seasonal behavior (maximum in May-June, minimum in December), which is consistent with reported results in the literature. Also, the polynomial fit curve in the last plot shows that the maximum in the ozone amount occurs in spring (April-May), which is in agreement with the expected seasonable change for the SGP location.

Comparison between this retrieval and the results obtained at the NYC site in 1995-1997 shows that the seasonal behavior of all retrieved quantities is essentially the same for both sites.

However, some geographical variability is present. AOD in NYC is slightly larger, while the particles are smaller (the same type of anti-correlation that was described above for the variability of these quantities in time). The average ozone amount is less for the SGP site, which reflects normal for ozone latitudinal variation. It seems rather unexpected that the  $\text{NO}_2$  column amount is quite similar for both sites, because NYC is an urban area and SGP is located in a rural district. This similarity is probably due to underestimation of the aerosol absorption for the SGP site discussed above, or may be due to some local sources of  $\text{NO}_2$  emission.

An interactive software with graphical interface was created to speed up the data processing (based on the algorithm described) and to establish effective control of the data on each step of the retrieval.

## References

- Alexandrov, M., A. A. Lacis, B. E. Carlson, and B. Cairns, 1997: Retrieval of aerosol optical depth, aerosol size distribution parameters, ozone and nitrogen dioxide column amounts from multifilter rotating shadowband radiometer data. In *Proceedings of the Seventh Atmospheric Radiation Measurement (ARM) Science Team Meeting*, CONF-970365, pp. 379-383. U.S. Department of Energy.
- Harrison, L., J. Michalsky, and J. Berndt, 1994: Automated multifilter shadow-band radiometer: instrument for optical depth and radiation measurement. *Appl. Opt.*, **33**, 5118-5125.
- King, M., and B. Herman, 1979: Determination of the ground albedo and the index of absorption of atmospheric particles by remote sensing. Part I: Theory. *J. Atmos. Sci.*, **36**, 163-173.

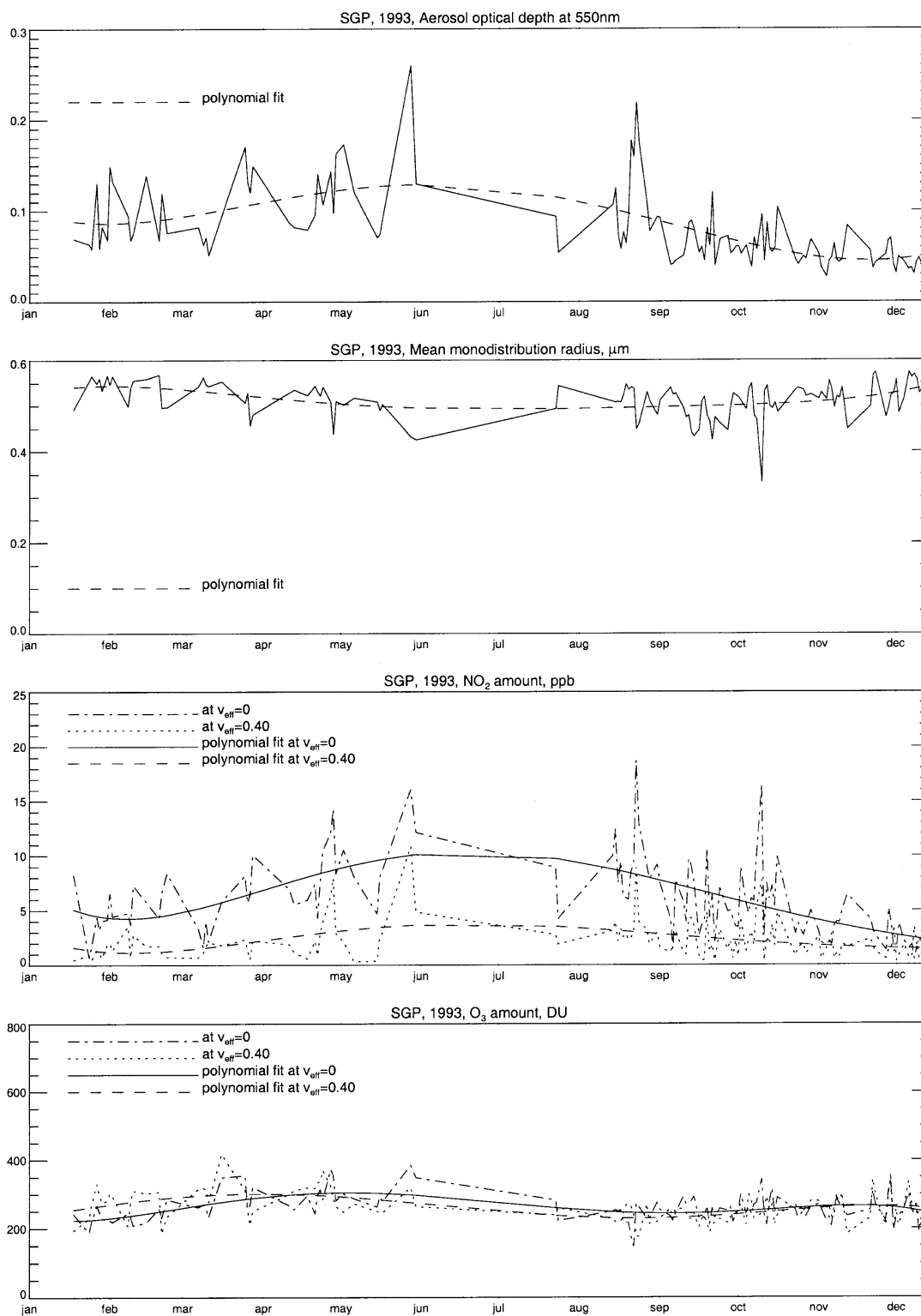


**Figure 1.** Retrieval analysis results for clear and partially clear days taken from MFRSR measurements at SGP in 1993.